Open Access, Peer Reviewed, Research Journal

Print & Online available on https://jesbulletin.in
Research Article

Synthesis and Characterization Copper Substituted Cobalt Ferrite by Standard Double Sintering Ceramic Technique

Yogesh G. Kute[1], Santosh. D. More[1], Mahesh. G. Shioorkar[2], Bhausaheb H. Devmunde[2,3]*

[1*]*Department of Physics, Deogiri College, Chhatrapati Sambhajinagar, 431005, MS, India*
[2]*Department of Physics, Vivekanand Arts, Sardar Dalipsingh Commerce and Science College, Chhatrapati Sambhajinagar, 431001 MS, India*

Corresponding author: bhdevmunde05@gmail.com

ARTICLE INFO

Received: 10/02/2024
Revised: 15/03/2024
Accepted: 01/04/2024

KEYWORDS

Cu- ferrites; XRD; Lattice parameter; FE-SEM; IR, Magnetization, etc.

ABSTRACT

A series of $Co_{1-x}Cu_xFe_2O_4$ with (x = 0.45) were synthesized by standard double sintering ceramic technique. The prepared samples have been pre-synthesized for 800 ^{0}c for 12 hrs and final sintering at 1100 ^{0}c for 16 hrs. The structural parameters were studied from XRD. The X-ray diffraction pattern at room temperature shows that the sample exists in single phase with a cubic spinel structure. From XRD data X-ray density, bond length and hopping length of the tetrahedral (A) site and octahedral (B) site were calculated. The lattice parameter (a) was determined to be 8.3685 Å, which is close to reported literature. The X-ray density (dx) of the prepared sample was recorded to be 5.3653 g/cm^3. FE-SEM was employed for morphological features of grain shape and grain size of mixed ferrite, $Co_{0.55}Cu_{0.45}Fe_2O_4$ powder. FT-IR curves shows two absorption bands ν_1 with higher frequency and ν_2 with lower frequency, indicating metal cation and oxygen bond stretching at tetrahedral and octahedral sites. The M-H loops revealed that the values of magnetic parameters such as Ms, Mr, Hc, η_B, and M_r/M_s ratio the saturation magnetization (M_s) increases with in copper substitution and remanent magnetization, coercivity field decrease.

1 Introduction

Cobalt ferrites are regarded as the best example of hard ferrite materials because of their exceptional chemical stability, mechanical hardness, appropriate saturation magnetization, and high magneto crystalline anisotropy [1]. The significantly impacted by magnetic ferrites applications in a wide range of fields, including the electrical and electronic industries, microwave and satellite communication technology, digital recording devices, and biomedical research [2]. There are numerous reports on Co – Cu ferrites synthesis in the literature M. A. Ahmed et al. [3] by ceramic technique, S. Saleem et al. [4] by sol-gel technique, N. Sanpo et al. [5] by sol-gel route, M. Hashim et al. [6] by sol-gel method, by chemical co-precipitation method synthesized samples. To study the in this paper $Co_{1-x}Cu_xFe_2O_4$ ferrites [7]. Cobalt ferrite ($CoFe_2O_4$) has a high cubic magneto crystalline anisotropy, moderate saturation magnetization and high coercivity [8]. At room temperature, cobalt ferrites have an inverse spinel structure with a high degree of inversion and show ferrimagnetism, with Co^{2+} ions occupying the octahedral B-sites and Fe^{3+} ions uniformly distributed across the tetrahedral A-sites and octahedral B-sites [9]. A ferrite is typically defined by the formula M (Fe_2O_4) where, M denotes any metal that forms divalent bonds, such as manganese (Mn^{2+}), nickel (Ni^{2+}), cobalt (Co^{2+}), zinc (Zn^{2+}), copper (Cu^{2+}), and magnesium (Mg^{2+}) [10]. The stoichiometry of these materials synthesis technique and sintering temperature are the effectively depend upon their structural, electrical, and magnetic properties [11]. These ferrimagnetic spinel ferrites are a significant family of magnetic ceramics that have an FCC crystal structure with oxygen ions arranged in 64 tetrahedral (A-Site) and 32 octahedral interstitial (B-Site) sites, with the metal cations occupying the remaining 32 (B-Site). The only that are 8 and 16 are occupied, respectively, by cations in stoichometric spinel. The metal cations occupy 8 of the tetrahedral (A-Site) and 16 of the octahedral (B-Site) sites out of this. Therefore, the significant amount of empty interstitial sites creates an open crystal structure that allows cations to move between interstitial sites during preparation [12]. These cobalt ferrite ceramics belong to a family that has received extensive research. Due to their high electromagnetic performance, good mechanical hardness, chemical stability, and high coercivity [13]. The present work is focused on the study of structural, SEM and IR properties and magnetization of $Co_{0.55}Cu_{0.45}Fe_2O_4$ prepared by standared double sintering ceramic technique.

II. Experimental details

II.I. Synthesis

The Copper substituted Cobalt ferrites with chemical formula $Co_{1-x}Cu_xFe_2O_4$ with composition (X = 0.45) were prepared by standard double sintering ceramic technique. The starting materials were 99.9 % (AR Grade) powders CoO, Fe_2O_3 and CuO were weighted in according to the stoichometric ratio. These stoichometric amounts of powder were mixed and grinded by mortar pestle. The grinded powders were pre-sintering at 800 ^oC for 12 hrs in a muffle furnace and slowly cooled to room temperature. After that the calcined powders were then grinded into the fine powders. The powders were finally sintering at 1100 ^oC for 16 hrs and slowly cooled to room temperature. After that the calcined powders were then grinded into the fine powders.

II.II. Characterization technique

The structural characterization of the ferrite powders was observed X-ray diffractometer by using a (Rigaku Miniflex sec.) with Cu Kα (Wavelengths λ = 1.5406 Å) radiation within angle range of the 20^0 to 80^0. The using a field-emission scanning electron microscopy and energy dispersive X-ray spectroscopy (EDX) images, samples of the surface morphology composition were produced (ZEISS). Infrared spectra was measured by using a fourier transform infrared (FTIR) spectrometer and wave numbers ranging from 400 to 800 cm^{-1} to determine the vibrations of ferrites (tetrahedral/octahedral) sites.

III. Results and discussion

III.I. X-ray diffraction study (XRD)

Fig. 1. Show that the XRD patterns of synthesis $Co_{1-x}Cu_xFe_2O_4$ with composition (X = 0.45) were single phase cubic spinel structure. The XRD pattern show that the following peaks at (30^0), (35^0), (37^0), (43^0), (53^0), (57^0), (62^0), (66^0), and (74^0) corresponding to the crystal planes of (220), (311), (222), (400), (422), (511), (440), (600), and (533) of the sample, which are in well agreement with already reported literatures [14,15]. All these peaks are the single phase FCC cubic spinel structure.

The lattice parameter of the sample was calculated by using the formula.

$$a = d\sqrt{h^2 + k^2 + l^2} \qquad (1)$$

Where, a is the lattice constant, (h, k, l) stands for the miller indices, and d is the inter planer spacing. An increase in lattice parameter of $Co_{1-x}Cu_xFe_2O_4$ is observed with the doping of Cu content in the lattice constant. The observed lattice constant increase 8.3685 Å. An increase in the lattice constant with increasing concentration of Co ionic radii (0.74 Å) are larger than that of Cu^{2+} ionic radii (0.70 Å) and Fe^{3+} (0.67 Å) ions obeying vegard's law. There is a relationship between the ionic radius and the lattice constant. As the lattice constant increase is proportional to the increase of the ionic radius [16].

The unit cell volume (V) was calculated by using the formula [17].

$$V = a^3\ Å \qquad (2)$$

Where, V is the unit cell volume, a is the lattice constant.

As the Cu content in the Co ferrite system increase, the unit cell volume (V) values gradually increase. The increase in lattice

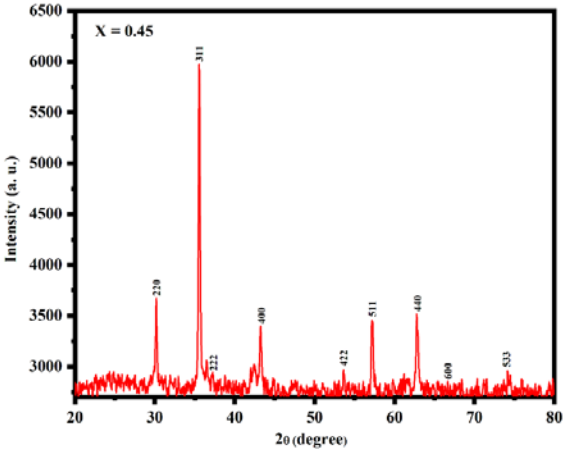

Fig. 1. XRD patterns of $Co_{0.55}Cu_{0.45}Fe_2O_4$ (x = 0.45) and ferrites

The crystallite size of the samples was calculated by using the Debye-Scherer's formula.

$$t = \frac{0.9\,\lambda}{\beta\ Cos\ \theta} \qquad (3)$$

Where, t is crystallite size, β is full width half maximum, θ is diffraction angle, and λ is the wavelength of the Cu-Kα radiation (λ = 1.5406 Å).

The crystallite size (t) was calculated from the FWHM of the peak with the highest intensity (311) [18]. Where, β = FWHM of the diffraction peak corresponding to the plane (311) [19]. λ is the X-ray wavelength of the considered as a Debye-Scherer's constant. It is observed that crystallite size decreases 39.35 nm. It is observed that crystallite size decrease with increasing Cu contents and Co contents were decreased.

The X-ray density of the sample was calculated by using the formula.

$$d_X = \frac{8\,M}{N\,a^3} \qquad (4)$$

Where, M is the molecular mass, N is Avogadro's number (N = 6.02×10^{23}), and a is the lattice constant. It was clear from Table 1. X-ray density increase with increasing Cu content 'x' 5.3653 g/cm^3. It is observed that X-ray density increase with increasing Cu content and Co content were decreased.

Table 1. lattice constant (a), Unit cell volume (V), Average crystallite size (D), X-ray density (dx), Tetrahedral (L_A) and Octahedral (L_B), for the $Co_{1-x}Cu_xFe_2O_4$ (X = 0.45).

(x)	a Å	(V) Å	D (nm)	dx (g/cm^3)	L_A Å	L_B Å
0.45	8.3685	586.0610	39.3505	5.3653	3.6235	2.9586

The hopping length tetrahedral A-site (L_A) and octahedral B-site (L_B) sites of the sample was calculated by using the formula.

$$L_A = a\frac{\sqrt{3}}{4}\ \text{Å} \quad (5)$$

$$L_B = a\frac{\sqrt{2}}{4}\ \text{Å} \quad (6)$$

The difference between the hopping lengths in the tetrahedral site (L_A) and the octahedral site (L_B). It is noted that the distance between the magnetic ions (hopping lengths) increases as Cu content 'x' increases. This behaviour of hopping length with 'x' is similar to that of 'a' with 'x', and it may be explained by the difference in the ionic radii of the component ions.

III.II. FTIR studies

The FTIR absorption bands of ferrite samples are attributed to the vibrations of the oxygen ions present in the tetrahedral and octahedral sites [20]. The FTIR absorption spectra of samples with wave numbers range from 400 to 800 cm^{-1} are given in fig. 2. [21]. The FTIR spectra exhibit two absorption band ν_1 524 cm^{-1} and ν_2 406 cm^{-1}, corresponding to intrinsic vibrations of tetrahedral and octahedral sites respectively. According to waldron's [22]. The tetrahedral sites are represented by the higher band ν_1 range from 500 to 550 cm^{-1} and octahedral sites by the lower band ν_2 in the range from 400 to 450 cm^{-1}. Which confirms the unit cell of single phase cubic spinel can be constructed in the tetrahedral (A) and octahedral (B) sites. According to IR absorption bond ν_1 can be assigned to stretching vibration of the tetrahedral (Me – O) metal – oxygen bond, and the absorption band ν_2 to the metal – oxygen vibrations in octahedral sites. The tetrahedral metal (Fe^{3+}) oxygen bond stretching vibrations are attributed for the absorption bond ν_1 and the metal Co^{2+} oxygen vibrations at the octahedral sites, are attributed for the absorption bond ν_2 [23].

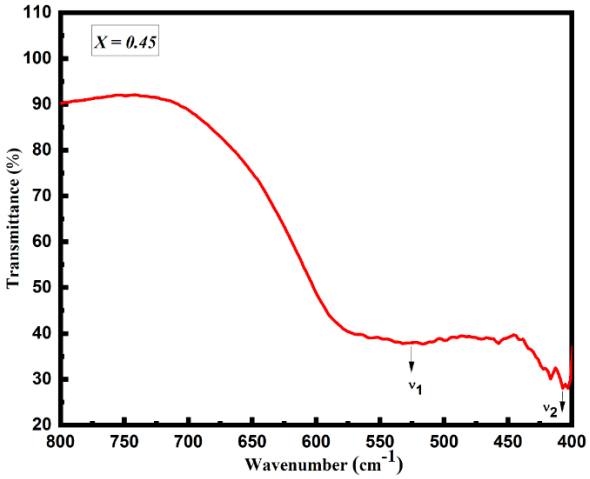

Fig. 2. FTIR spectra for $Co_{0.55}Cu_{0.45}Fe_2O_4$ ferrites.

III.III. Fe-SEM

Fig. 3. The Fe-SEM micrograph of $Co_{1-x}Cu_xFe_2O_4$ ferrite nanoparticles. The surface morphological image at 5.00 Kx magnifications was collected. The Fe-SEM micrograph of the synthesized $Co_{1-x}Cu_xFe_2O_4$ ferrite nanopowders. Fine grain growth is found in the sample by a closer look at these microstructures, it is found that the grains in the sample are spherical shape and the agglomeration increases with increasing copper content.

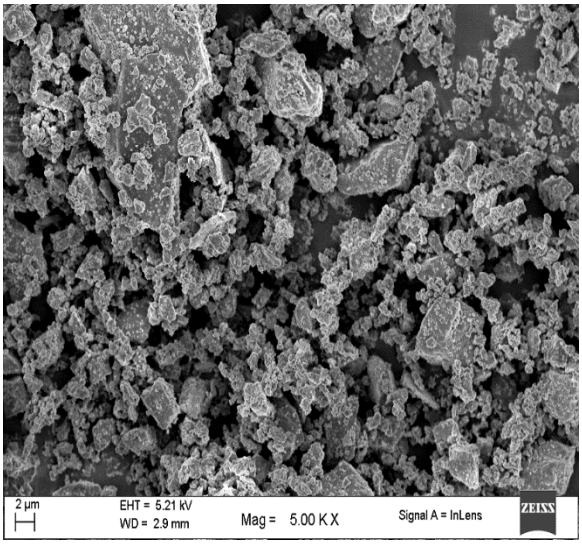

Fig. 3. Fe-SEM micrograph of the $Co_{1-x}Cu_xFe_2O_4$ sample (X = 0.45).

III.IV. Energy – dispersive X-ray spectroscopy (EDX)

The sample of $Co_{1-x}Cu_XFe_2O_4$ ferrite nanoparticles with (X = 0.45) was carried out by Energy – dispersive X-ray spectroscopy. Fig. 4. The presence of Co, Cu, Fe and O elements peaks observed in the EDX spectrum which indicates the purity of the $Co_{1-x}Cu_XFe_2O_4$ ferrite nanoparticles sample. This result indicates that the obtained atomic ratio of all elements (Co, Cu, Fe and O) was well matched in synthesized nanoparticles.

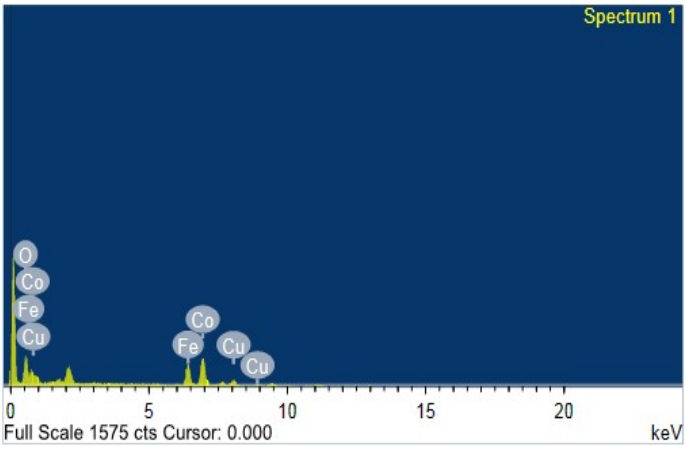

Fig. 4. EDX image of the $Co_{1-X}Cu_XFe_2O_4$ sample (X = 0.45)

III.V. Magnetic measurement

Fig. 5. Shows the hysteresis loop for $Co_{1-X}Cu_XFe_2O_4$ ferrite it shows the magnetization versus applied field (M-H) curve of the synthesized sample obtained by using a vibrating sample magnetometer (VSM) at room temperature. The values of various magnetic parameters such as saturation magnetization (M_s), remanent magnetization (M_r) and coercivity (H_c) were measured to be 59.89 emu/g, 10.10 emu/g and 0.2041 Oe and the values are shown in table (2).

The values of magnetic parameters M_s, M_r, and H_c, M_r/M_s and η_B of $Co_{1-X}Cu_XFe_2O_4$ nanoparticles at X = 0.45.

X	Saturation magnetization M_s (emu/g)	Remanent magnetization M_r (emu/g)	Coercivity H_c (Oe)	M_r/M_s	Magnetic moment $\eta_B(\mu_B)$	K (erg/g)
0.45	59.89	10.10	0.2041	0.1686	3.5164	12.7328

Magnetic interactions and cation distribution in the tetrahedral and octahedral sites have been shown to influence the structural and magnetic properties of spinel ferrites [24]. Therefore, the magnetic exchange interactions and cation distribution are varied by increasing the Co/Cu concentration ratio, resulting in a change in magnetic properties. The ideal spinel structure has two sub-lattices, namely tetrahedral (A) and octahedral (B) sites. The magnetic properties of spinel ferrite are primarily determined by the different combinations of metal cation charges that are distributed between the sites A and B. The magnetic moment in ηB per formula unit following is computed using the relation.

$$\eta B = \frac{Ms * Mw}{5585} \qquad (7)$$

Where M_s = Saturation magnetization and M_w = Molecular weight, the magnetic moment η_B was found to be 3.5164. The magnetic anisotropy (K) is estimated by the following relation [27].

$$K = \frac{Ms*Hc}{0.96} \qquad (8)$$

Where H_c and M_s is coercivity, saturation magnetization respectively. The magnetic anisotropy (K) value was 12.7328 erg/g.

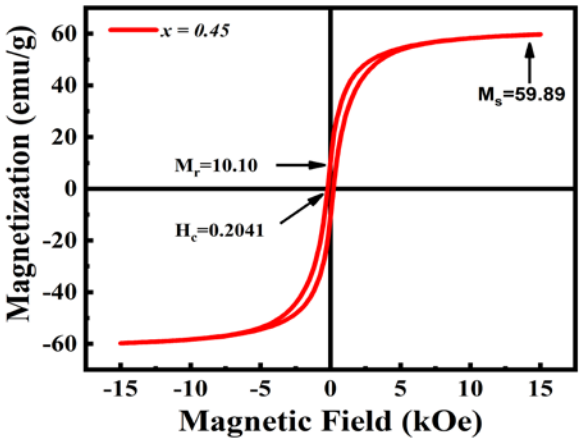

Fig. 5. Magnetization hysteresis loop of $Co_{1-X}Cu_XFe_2O_4$ sample (X = 0.45)

IV. Conclusion

The sample of $Co_{1-X}Cu_xFe_2O_4$ ferrite nanoparticles with (X = 0.45) were successfully synthesized by standard double sintering ceramic technique. The X-ray diffraction pattern reveals the confirmation of single phase cubic spinel structure. The lattice parameter increases with increasing the copper content. The crystallite size decrease with increasing the copper content. Structural parameters such as lattice parameters and X-ray density increase with increasing the Copper content. Two absorption peaks near ν_1 524 cm^{-1} and ν_2 406 cm^{-1} observed in FTIR spectra which confirmed the ferrite nature of the sample. The Fe-SEM micrograph shows the spherical shape of grains and the agglomeration increases with increasing copper content. The presence of Co, Cu, Fe, and O elements in the ferrite samples were confirmed from EDX measurements. The magnetic properties have been analyzed, which confirms the ferrimagnetic behaviour. The saturation magnetization (M_s) increases with in copper substitution and remanent magnetization, coercivity field decrease.

V. References

[1] M. Z. Ahsana and F. A. Khan, Study of structural, electrical and magnetic properties of manganese doped cobalt ferrite nanoparticles with non-stoichiometric composition. Journal of Physical Science and Application, Vol. 7 (6) PP. 30-37, 2017.

[2] M. Sugimoto, The past, present and future of ferrites, Journal of the American Ceramic Society, Vol. 82, PP. 269-280, 1999.

[3] M. A. Ahmed, S. F. Mansour and M. A. Abdo, Characterization and dramatic variations of the magnetic properties of Cu-doped

nanometric Co ferrite. Physica Scripta, Vol. 84, PP. 5, 055602, 2011.

[4] S. Saleem, M. Irfan, M. Y. Naz, S. Shukrullah, M. A. Munir, M. Ayyaz, A. S. Alwadie, S. Legutko, J. Petru, and S. Rahman, Investigating the impact of Cu^{2+} doping on the morphological, structural, optical, and electrical properties of $CoFe_2O_4$ nanoparticles for use in electrical devices. MDPI, Vol. 15(10): 3502, 2022.

[5] N. Sanpo, J. Wang and C. C. Berndt, Sol-gel synthesized copper-substituted cobalt ferrite nanoparticles for biomedical applications. Journal of Nano Research, Vol. 22, PP. 95-106, 2013.

[6] M. Hashim, Alimuddin, S. Kumar, B. H. Koo, S. E. Shirsath, E. M. Mohammed, J. Shah, R. K. Kotnala, H. K. Choi, H. Chung, R. Kumar, Structural, electrical and magnetic properties of Co-Cu ferrite nanoparticles. Journal of Alloys and Compounds, Vol. 518, PP. 11-18, 2012.

[7] M. Margabandhu, S. Sendhilnathan, S. Senthilkumar, D. Gajalakshmi, Investigation of structural, morphological, magnetic properties and biomedical applications of Cu^{2+} substituted uncoated cobalt ferrite nanoparticles. Biological and Applied Sciences, Vol. 59, ISSN 1678-4324, 2016.

[8] T. Mariam, I. N. Esha, M. N. I. Khan, S. Choudhary and K. H. Maria, Synthesis of zinc substituted cobalt ferrites via standard double sintering ceramic technique: A study on their structural, magnetic and dielectric properties. Journal of Ceramic Processing Research, Vol. 21, No. 4, PP, 442-449, 2020.

[9] R. Zhang, L. Sun, Z. Wang, W. Hao, E. Cao, Y. Zhang, Dielectric and magnetic properties of $CoFe_2O_4$ prepared by sol-gel auto-combustion method. Journal of Materials Research Bulletin, PII: S0025-5408 (17) 3017-8, 2017.

[10] P. P. Khine, M. S. Myint and W. Kyaw, Study on characterization of $Mg_{0.5}Cu_{0.5}Fe_2O_4$ ferrite compound. Journal of the Myanmar Academy of Arts and Science, Vol. 16, No. 2, 2018.

[11] B. H. Devmunde, P. S. Bhalerao, M. B. Solunke, Structural morphological and infrared properties of Cd^{2+} substitutes nickel ferrite particles. Journal of Physics, Vol. 1644, 012021, 2020.

[12] M. A. Khan, M. J. ur Rehman, K. Mahmood, I. Ali, M. N. Akhtar, G. Murtaza, I. Shakir, M. F. Warsi, Impacts of Tb substitution at cobalt site on structural, morphological and magnetic properties of cobalt ferrites synthesized via double sintering method. Ceramics International, Vol. 41, PP. 2286-2293, 2015.

[13] S. Wells, C. V. Ramana, Effect of hafnium-incorporation on the microstructure and dielectric properties of cobalt ferrite ceramics. Ceramics International, Vol. 39, PP. 9549-9556, 2013.

[14] H. Kumar, R. C. Srivastava, J. P. Singh, P. Negi, H. M. Agrawal, D. Das and K. Hwachae, Structural and magnetic properties of dysprosium substituted cobalt ferrite nanoparticles. Journal of Magnetism and magnetic materials, Vol. 401, PP. 16-21, 2015.

[15] N. Ponpandian, P. Balaya and A. Narayanasamy, Electrical conductivity and dielectric behaviour of nanocrystalline $NiFe_2O_4$ spinel. Journal of Physics: Condensed Matter Vol. 14, PP. 3221-3237, 2002.

[16] A. Poddar, S. Halder, S. I. Liba, S. M. Hoque and S. S. Sikder, Study of the quenching on microstructural and magnetic properties of Cu-doped Mg-ferrite. Advances in Condensed Matter Physics, Vol. 2022, PP.10.

[17] X. Wang, X. Kan, X. Liu, S. Feng, G. Zheng, Z. Cheng, W. Wang, Z. Chen, C. Liu, Characterization of microstructure and magnetic properties for Co^{2+} ions doped $MgFe_2O_4$ spinel ferrites. Materials Today Communications, Vol. 25, 1011414, 2020

[18] S. K. Sen, V. C. Barman, M. Manir, P. Mondal, S. Dutta, M. Paul, M. Chowdhury, M. Hakim, X-ray peak profile analysis of pure and Dy-doped α-MoO_3 nanobelts using Debye-Scherrer, Williamson-Hall and Halder-Wagner methods, Adavances in Natural Sciences: Nanoscience and Nanotechnology, Vol. 11, 025004, 2020.

[19] S. Talam, S. R. Karumuri, N. Gunnam, Synthesis characterization and spectroscopic properties of ZnO nanoparticles. International Scholarly Research Notices, 2012.

[20] S. A. Mazen and T. A. Elmosalami, Structural and elastic properties of Li-Ni ferrite. ISRN Condensed Matter Physics, Vol. 2011, PP. 9, 820726.

[21] P. B. Belavi, G. N. Chavan, L. R. Naik, R. Somashekar, R. K. Kotnala, Structural, electrical and magnetic properties of cadmium substituted nickel-copper ferrites. Materials Chemistry and Physics, Vol. 132, PP. 138-144, 2012.

[22] R. D. Waldron, Infrared spectra of ferrites, Physical Review, Vol. 99, No. 6, PP. 1727-1735, 1955.

[23] A. S. Pujar, A. B. Kulkarni, S. N. Mathad, C. S. Hiremath, M. K. Rendale, M. R. Patil, and R. B. Pujar, Structural, electrical, and IR properties of $Cu_xCo_{1-x}Fe_2O_4$ (x = 0, 0.4, 1.0) prepared by solid-state method. ISSN 1061-3862, International Journal of Self-Propagation High-Temperature Synthesis, Vol. 27, No. 3, PP. 174-179, 2018.

[24] Talaat M. Hammad, S. Kuhn, Ayman Abu Amsha, Nasser K, Hejazy, R. Hempelmann, Comprehensive study of the Impact of Mg2+ Doping on Optical, Structural and magnetic Properties of Copper Nanoferrites. Journal of Superconductivity and Novel magnetism (2020).

[25] Dhanraj Aepurwar, Yogesh Kute, D. R. Shengule, B. H. Devmunde, Effect of Cd2+ on the Structural and Magnetic Properties of Lithium-Nickel Ferrite Nanooarticles. International Journal of Scientific Research in Science and Technology, Vol. 11, PP. 66-70, 2024.